Diode Equivalent Parameters of Solar Cell

Sk Md Iftiquar[1)]* · Vinh Ai Dao[1)] · Junsin Yi[1,2)]*

[1)]College of Information and Communication Engineering, Sungkyunkwan University, Suwon, 16419, Republic of Korea,
[2)]Department of Energy Science, Sungkyunkwan University, Suwon, 16419, Republic of Korea

ABSTRACT: Current characteristic curve of an illuminated solar cell was used to determine its reverse saturation current density (J_0), ideality factor (n) and resistances, by using numerical diode simulation. High efficiency amorphous silicon, heterojunction crystalline Si (HIT), plastic and organic-inorganic halide perovskite solar cell shows n=3.27 for a-Si and n=2.14 for improved HIT cell as high and low n respectively, while the perovskite and plastic cells show n=2.56 and 2.57 respectively. The J_0 of these cells remain within 7.1×10^{-7} and 1.79×10^{-8} A/cm^2 for poorer HIT and improved perovskite solar cell respectively.

Key words: Amorphous silicon solar cell, Diode equivalent model, Numerical method, Active layer defect density

Nomenclature

J_0 : reverse saturation current density, A/cm^2
n : ideality factor
R_s : series resistance, $\Omega.cm^2$
R_p : shunt resistance, $\Omega.cm^2$
N_d : defect density, cm^{-3}
V_{oc} : open circuit voltage, Volts
J_{sc} : short circuit current density, mA/cm^2
FF : fill factor
Eff : efficiency, %
P_{maxV} : voltage at maximum power point, mV
P_{maxJ} : current density at maximum power point, mA/cm^2

Subscript

AFORS HET : Automat for simulation of heterostructure
HIT : heterojunction with intrinsic thin layer
SKE : stacked emitter
SE : single emitter
a-Si : amorphous silicon
J-V : current density voltage
p-a-SiO:H : p-type hydrogenated amorphous silicon oxide
i-a-SiO:H : intrinsic hydrogenated amorphous silicon
n-a-SiO:H : n-type hydrogenated amorphous silicon
q : charge of electron
k : Boltzmann constant
T : temperature

1. Introduction

Solar cell can be modeled as a combination of diode and resistor in absence of light, while in presence of incident light a certain constant current source should be added in the equivalent circuit[1-4)]. Energy of the current source comes from incident light, because the solar cell can convert light into electrical energy. The diode current changes non-linearly with applied electrical bias, that makes the solar cell a bit complicated to analyze or evaluate its diode ideality factor (n), reverse saturation current density (J_0), series (R_s) and shunt (R_p) resistances. Attempts to find these characteristic solar cell parameters can be found as early as 1981[5)] to until recently in 2015[6,7)]. Different authors propose different techniques like analytical[1,8-14)], numerical[15-17)], experimental[6,18,19)] methods etc. However, most of these techniques are either difficult to adapt or time consuming to implement.

The quickest and one of the most popular approaches is to evaluate dynamic series and shunt resistances from a slope of the illuminated current density vs voltage characteristic (J-V) curve near open circuit and short-circuit conditions respectively, however, it was suggested that this method of estimating the resistances may not be good[20)]. Here we propose a simple numerical simulation technique to determine these diode parameters.

*Corresponding author: iftiquar@skku.edu, yi@yurim.skku.edu
Received October 21, 2015; Revised November 23, 2015; Accepted December 4, 2015

2. Theoretical

When light is incident on a solar cell it generates electricity at the expense of photon. This generation of electricity can be denoted as a current source (J_{scm}), where the maximum current density, which is short circuit current density (J_{sc}), available from the solar cell can be J_{scm}. We use a conventionally used equivalent circuit model in our analysis[21], as shown in Fig. 1. The output current density can be written with the help of Shockley diode equation, as is given in equation (1). We solve this equation numerically for the constant parameters.

$$J = J_{scm} - J_0\left[e^{\left(\frac{qV+qJR_s}{nkT}\right)} - 1\right] - \frac{V+JR_s}{R_p} \quad (1)$$

3. Computational Details

Initial values of the constants can be obtained from the following equations:

$$J_0 = \frac{J_{scm}}{e^{qVoc/nkT} - 1} \quad (2)$$

$$R_s = -\left.\frac{\Delta V}{\Delta J}\right|_{V \to Voc} \quad (3)$$

$$R_p = -\left.\frac{\Delta V}{\Delta J}\right|_{V \to 0} \quad (4)$$

$$J_{sc} = J_{scm} = J|_{V \to 0} \quad (5)$$

$$n \approx 1.5 \quad (6)$$

Fig. 2 shows the flowchart of the numerical simulation steps. After a testing phase we observed that a 100 cycle of iterations can result in a reasonably acceptable solution. A step by step evolution of the solutions is shown below. We have noticed that the final acceptable solution does not depend on the initial guesses, obtained from equations (2)-(6).

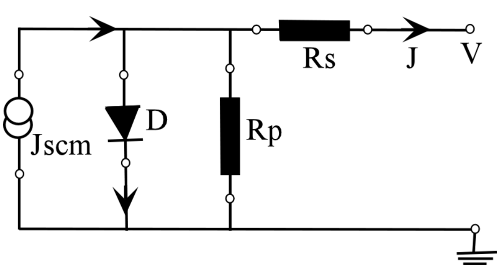

Fig. 1. The single diode equivalent circuit of a solar cell

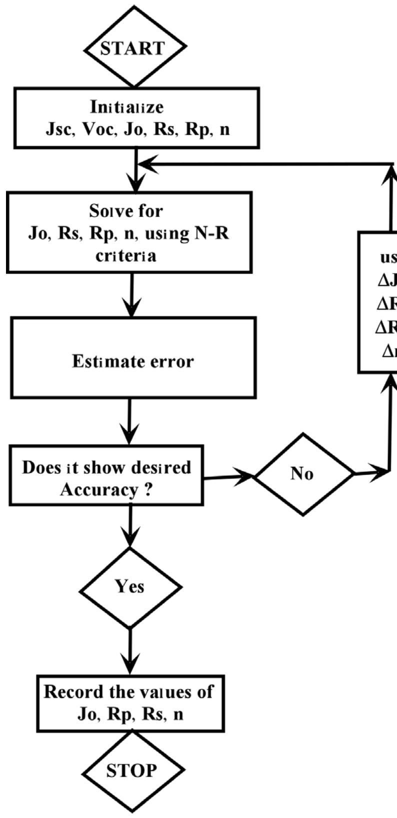

Fig. 2. Flowchart of the simulation, N-R criteria is the Newton-Raphson criteria

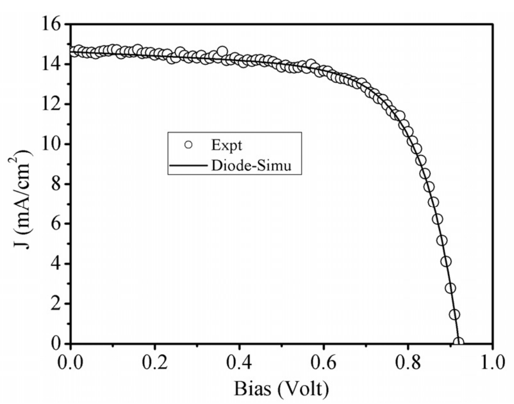

Fig. 3. Current density, J(mA/cm^2) vs bias voltage plot of the reference cell denoted by symbols, and continuous line as diode simulation

In the following we describe outcome the simulation and its evolution with iteration cycle, with the help of a J-V characteristic curve, published in reference[22], as shown in Fig. 3. In this figure a good match of the simulation to the experimental results can be observed. This final solution appears after 100 iteration cycles. Graphical evolution of the solutions are shown in Fig. 4.

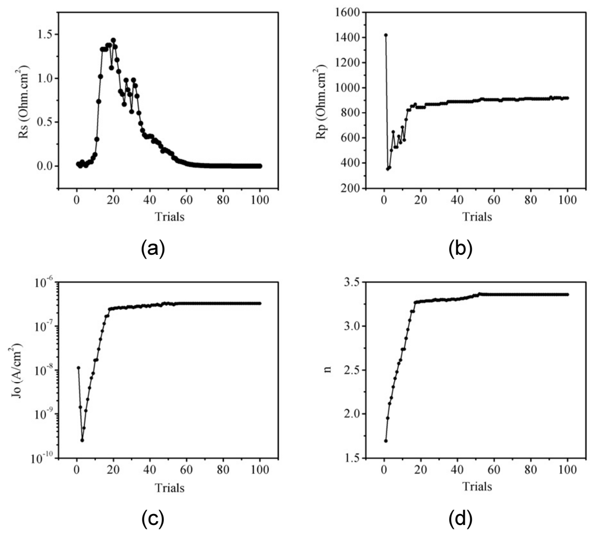

Fig. 4. Evolution of parameters with number of trials during diode simulation of (a) series resistance, R_s, (b) shunt resistance, R_p, (c) reverse saturation current density, J_0, (d) diode ideality factor, n

Table 1. Extracted solar cell parameters from some of the published results, as indicated in "Ref" column of the table. R_s of these cells lie within a small range of 0.001 to 0.0015 Ω.cm^2. HIT indicates silicon hetero-junction solar cell with intrinsic thin amorphous silicon passivation layer, SKE is stacked emitter, SE is single emitter, Perovskite implies Perovskite with 180 μ grain

R_p (Ω. cm^2)	n	J_0 (A/cm^2)	Cell type	Ref
918	3.27	3.4×10^{-7}	a-Si	[22], Fig. 5B
3000	2.14	1.16×10^{-7}	HIT, SKE	[23], Fig 3(b)
312	2.49	7.1×10^{-7}	HIT, SE	[23], Fig 3(b)
700	2.56	1.79×10^{-8}	Perovskite	[24], Fig. 2B
206	2.57	3.64×10^{-8}	Plastic	[25,26], Fig. 2 of [25]

4. Results and Discussions

We used a-Si, Si heterojunction (HIT), plastic and organic inorganic halide perovskite solar cells, and evaluated their characteristic parameters. The results are given in Table 1.

Shunt resistance, as shown in Fig. 1, can also be understood as the leakage resistance. In the device fabrication process, if the cathode and anode are not insulated well then a part of the device output leaks without contributing to the load current. Therefore higher R_p is preferable. Here we obtained 3 kΩ.cm^2 as the highest and 206 Ω.cm^2 as the lowest R_p for a HIT cell and plastic cell respectively. Thus, as it appears from the above results, a significant ohmic leakage exists in most of the above cells. The $n > 2$ indicates, that the equivalent diode of the solar cells are not an ideal one, as $n = 1$ for an ideal diode. The J_0 may indicate the

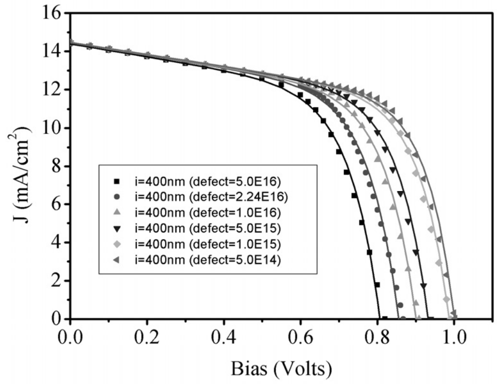

Fig. 5. J-V characteristics of the cells with varying i-layer defect density, the data points are the results of AFORS-HET simulation, adopted from reference[27], while the continuous lines are the numerical diode simulation based on the equation (1), as described above

recombination loss of charge carriers[19], so higher J_0 may imply that total defects in the active layer is relatively high because of which more photo carriers are lost by recombination. Table-I shows that, for a-Si solar cell the J_0 is smaller than that of the HIT cell (with single emitter, HIT SE), but higher than that of a perovskite solar cell. From this point of view, the organic-inorganic halide perovskite solar cell may have a lower recombination loss, but here the ohmic leakage is higher than that in a-Si or HIT solar cell (SKE).

The parameters given in Table I are for different types of solar cells. In order to have a better understanding of these parameters, we use the J-V characteristics of the cell from reference[27] (Fig. 7(a), trace "Simu1" of Ref[27]). This cell structure was p-a-SiO:H (20nm)/i-a-Si:H(225 nm)/n-a-Si:H(25 nm) and defect density as 8×10^{17} cm^{-3} [27], without surface texture and back reflector. Additional J-V characteristic curves, used for the investigation here, were obtained by AFORS HET simulation and for various lower defect densities (details of the simulation can be found in reference[27]). Some of the results are given below.

It is to be noted that the short circuit current density (J_{sc}) of these cells in Fig. 5, remains constant while the open circuit voltage (V_{oc}) increases with reduced defect density. Some of the cell parameters are shown in Fig. 6.

These are for solar cells that have 400 nm thick active layer, but with a varying defect density. J_{sc} of all the cells remain 14.4 (±0.05) mA/cm^2 , with P_{maxJ} = 11.4(±0.1) mA/cm^2, R_p = 311(±9) Ω.cm^2. The n remained 3.0 for all the cells except the last one with 2.8 ($N_d = 5\times10^{14}$ cm^{-3}).

The Fig. 6 shows the variation in cell characteristic parameters

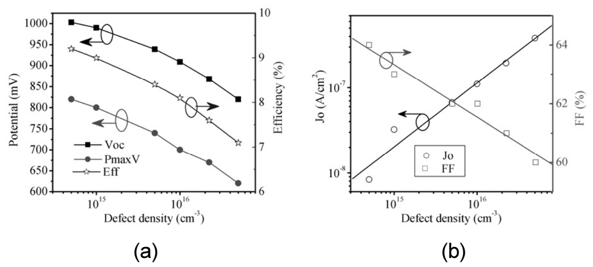

Fig. 6. Variation of characteristic parameters of solar cells that differ in defect density in the active layer. (a) Variation of V_{oc}, P_{maxV} and efficiency, (b) reverse saturation current density and FF

when defect density of the active layer was varied. The interesting thing to note here is that with the change in defect density in the range of N_d = 5×10^{16} to 5×10^{14} cm^{-3}, the reverse saturation current density J_0 reduces, keeping other diode equivalent parameters as mostly unchanged. It is significant and a clear indication that J_0 strongly depends upon defect density[19]. Furthermore, Fig. 6(a) shows that the P_{maxV}, V_{oc} and efficiency (Eff) increases almost logarithmically with the reduction in defect density. Similarly the Fig. 6(b) shows that the FF reduces logarithmically while the J_0 increases linearly with the increase in defect density. In respect to other parameters, it is to be noticed here that the R_p remains nearly constant while the FF decreases as a result of increased N_d of the active layer. Therefore a common perception[28] that the FF changes due to change resistance or energy band structure at the device interfaces, may not always be true. Furthermore, the resistance obtained from local slope of J-V curve is a dynamic resistance (changes from one measurement point to another), which is different from the resistances obtained by the diode simulation and reported here.

It seems that the cells with higher J_0 or n may degrade faster, because they are most likely to have higher defect density. It can be noticed from the results of this work as well as reference[19], these cells are expected to have higher defect density in the active layer. As a result of this, the degradation of these cells is expected to be higher. Therefore, some information regarding stability of a cell can be obtained from these J_0 and n, where improved cells may need to have lower J_0 and n.

5. Conclusions

Numerical diode simulation can give a reliable solution of the modified Shockley diode equation of a solar cell. A good test of reliability of the solution is that the simulated J-V characteristic curve will be very much similar to the reference data, and numerical values of unknown parameters will not change much for subsequent iterations. The value of the resistances obtained in this method corresponds to static resistances. Increased J_0 and n indicates that diodic nature of the cell is poorer, yet it may be possible that some of these cells exhibit higher initial efficiency but poorer stability.

Acknowledgments

This work was supported by the New & Renewable Energy Core Technology Program of the Korea Institute of Energy Technology Evaluation and Planning (KETEP) granted financial resource from the Ministry of Trade, Industry & Energy, and Republic of Korea (No. 20133030010930).

This work was supported by the Human Resources Development program (No. 20144030200580) of the Korea Institute of Energy Technology Evaluation and Planning (KETEP) grant funded by the Korea government Ministry of Trade, Industry and Energy.

References

1. J.C.H. Phang, D.S.H. Chan, J.R. Phillips, "Accurate analytical method for the extraction of solar cell model parameters", Electron. Lett., 20 (1984) 406-408.
2. D.S.H. Chan, J.R. Phillips, J.C.H. Phang, "A comparative study of extraction methods for solar cell model parameters", Solid State Electronics, 29 (1986) 329-337.
3. X. Yuan, Y. He, L. Liu, "Parameter extraction of solar cell models using chaotic asexual reproduction optimization", Neural Comput. Appl., (2014).
4. J. Cabestany, L. Castaner, "Evaluation of solar cell parameters by nonlinear algorithms", Journal of Physics D: Applied Physics, 16 (1983) 2547-2558.
5. J.P. Charles, M. Abdelkrim, Y.H. Muoy, P. Mialhe, "A practical method of analysis of the current-voltage characteristics of solar cells", Solar Cells, 4 (1981) 169-178.
6. T. Sogabe, A. Ogura, M. Ohba, Y. Okada, "Self-consistent electrical parameter extraction from bias dependent spectral response measurements of III-V multi-junction solar cells", Prog Photovoltaics Res Appl, 23 (2015) 37-48.
7. K. Tada, "Parameter extraction from S-shaped current-voltage characteristics in organic photocell with opposed two-diode model: Effects of ideality factors and series resistance", Phys. Status Solidi A Appl. Mater. Sci., (2015).
8. D.S.H. Chan, J.C.H. Phang, "Analytical methods for the extraction of solar-cell single- and double-diode model parameters from i-v characteristics", IEEE Trans. Electron Devices,

ED-34 (1987) 286-293.

9. J. Merten, J.M. Asensi, C. Voz, A.V. Shah, R. Platz, J. Andreu J Merten, J.M. Asensi, C. Voz, J. Andreu, "Improved equivalent circuit and analytical model for amorphous silicon solar cells and modules", IEEE Trans. Electron Devices, 45 (1998) 423-429.
10. H. Saleem, S. Karmalkar, "An analytical method to extract the physical parameters of a solar cell from four points on the illuminated J-V curve", IEEE Electron Device Letters, 30 (2009) 349-352.
11. A.K. Das, S. Karmalkar, "Analytical derivation of the closed-form power law J-V model of an illuminated solar cell from the physics based implicit model", IEEE Trans. Electron Devices, 58 (2011) 1176-1181.
12. H. Fathabadi, "Novel neural-analytical method for determining silicon/plastic solar cells and modules characteristics", Energy Convers. Manage., 76 (2013) 253-259.
13. V. Lo Brano, G. Ciulla, "An efficient analytical approach for obtaining a five parameters model of photovoltaic modules using only reference data", Appl. Energy, 111 (2013) 894-903.
14. J. Cubas, S. Pindado, M. Victoria, "On the analytical approach for modeling photovoltaic systems behavior", J Power Sources, 247 (2014) 467-474.
15. T.K.P. Wong, P.C.H. Chan, An equivalent circuit model approach to the numerical modelling of a p-n solar cell and photodetector, Int J Optoelectron, 11 (1997) 29-38.
16. J. Villanueva, J.A. Anta, E. Guillén, G. Oskam, "Numerical simulation of the current-voltage curve in dye-sensitized solar cells", J. Phys. Chem. C, 113 (2009) 19722-19731.
17. W. Ding, R. Jia, D. Wu, C. Chen, H. Li, X. Liu, T. Ye, "Numerical simulation and modeling of spectral conversion by silicon nanocrystals with multiple exciton generation", J Appl Phys, 109 (2011).
18. E. Cuce, P.M. Cuce, T. Bali, "An experimental analysis of illumination intensity and temperature dependency of photovoltaic cell parameters", Appl. Energy, 111 (2013) 374-382.
19. H. Sakai, T. Yoshida, S. Fujikake, T. Hama, Y. Ichikawa, "Effect of p/i interface layer on dark J-V characteristics and Voc in p-i-n a-Si solar cells", J Appl Phys, 67 (1990) 3494-3499.
20. S. Voswinckel, V. Wesselak, B. Lustermann, "Behaviour of amorphous silicon solar modules: A parameter study", Sol. Energy, 92 (2013) 206-213.
21. L. Peng, Y. Sun, Z. Meng, "An improved model and parameters extraction for photovoltaic cells using only three state points at standard test condition", J Power Sources, 248 (2014) 621-631.
22. K. Yoon, Y. Kim, J. Park, C.H. Shin, S. Baek, J. Jang, S.M. Iftiquar, J. Yi, "Preparation and characterization of p-type hydrogenated amorphous silicon oxide film and its application to solar cell", J Non Cryst Solids, 357 (2011) 2826-2832.
23. Y. Lee, H. Kim, S.M. Iftiquar, S. Kim, S. Kim, S. Ahn, Y.J. Lee, V.A. Dao, J. Yi, "Study of stacked-emitter layer for high efficiency amorphous/crystalline silicon heterojunction solar cells", J Appl Phys, 116 (2014).
24. W. Nie, H. Tsai, R. Asadpour, J.C. Blancon, A.J. Neukirch, G. Gupta, J.J. Crochet, M. Chhowalla, S. Tretiak, M.A. Alam, H.L. Wang, A.D. Mohite, "High-efficiency solution-processed perovskite solar cells with millimeter-scale grains", Science, 347 (2015) 522-525.
25. A. Ortiz-Conde, F.J. García Sánchez, J. Muci, "New method to extract the model parameters of solar cells from the explicit analytic solutions of their illuminated I-V characteristics", Sol Energ Mater Sol Cells, 90 (2006) 352-361.
26. T. Jeranko, H. Tributsch, N.S. Sariciftci, J.C. Hummelen, "Patterns of efficiency and degradation of composite polymer solar cells", Sol Energ Mater Sol Cells, 83 (2004) 247-262.
27. S.M. Iftiquar, J. Jung, C. Shin, H. Park, J. Park, J. Jung, J. Yi, "Light management for enhanced efficiency of textured n-i-p type amorphous silicon solar cell", Sol Energ Mater Sol Cells, 132 (2014) 348-355.
28. K.W. Mitchell, A.L. Fahrenbruch, R.H. Bube, "Analysis of the fill factor for n-CdS/p-CdTe solar cells", Solid-State Electron., 20 (1977) 559-561.